Al-Qadisiyah Journal of Veterinary Medicine Sciences
(P-ISSN 1818-5746/ E-ISSN 2313-4429)
www.qu.edu.iq/journalvm

Turmeric extracts nanoparticles ointment for treatment of infected open wounds

Laith Mohanad Jabbar[1] and Thaier Alwan Abid[1*]
[1]Department of Surgery and Obstetric, College of Veterinary Medicine, University of Al-Qadisiyah, Al-Diwaniyah, Iraq
***Correspondence: Thaier.abid@qu.edu.iq**

Abstract

To investigate the effects of topical application of turmeric extract nanoparticles ointment in treatment of infected wounds in mice. Thirty male mice had been divided into two groups, G1 (control) and G2 (treated). Two circular (0.5cm) full thicknesses skin wounds were performed on the animal's back. After 24 hours after wounding 0.2 mL of a *Pseudomonas aeruginosa* bacterial suspension containing $2x10^8$ CFU/mL of bacteria was injected in the right wounds to cause infection. The left wounds wasn't injected or treated and consider as a negative control in the same animal. Wounds of G1 were not treated after receiving a bacterial inoculation. Infected wounds of G2 were treated with a topical application of 3% turmeric extract nanoparticle ointment at a dose of $30mg/cm^2$ once daily for seven consecutive days. Healing was evaluated by measuring the size of the wound and by histopathology samples taken at 7 and 14 days PI**.** At the 7^{th} day PI the size of infected non-treated wounds in G1 (129.35%) was become significantly $P < 0.05$ larger than the original size, while the treated wounds in G2 were significantly $P < 0.05$ reduced more than 45.25% in compare with initial wound size. At the 14^{th} day PI the size of infected non-treated wounds in G1 (174.66%) was significantly $P < 0.05$ larger than the original size, with no healing, while in G2 the reduction in size become significantly (32.36%) smaller. The percentage of wound contraction was significantly increased ($P < 0.05$) in treated wounds at 7^{th} and 14^{th} days as compared with no wound contraction (0%) in G1. Histopathologically the infected wounds in G1 at 7^{th} and 14^{th} day PI exhibit an absence of epithelial layers, suppurative exudate, dead liquefied tissue, and an abundance of both dead and living neutrophils. G2 at 7^{th} day PI display, no evidence of infection, fully epithelialized epidermis, and immature granulation tissue are visible. On the 14^{th} day PI revealed a well-regenerated epidermis, and mature collagen fibers with myofibroblast in the dermis. The treatment of infected wounds with turmeric extract nanoparticles ointment 3% improved the healing process and accelerated the proliferation, wound contraction, maturation, and remodeling phases of wound healing.

Keywords: Curcumin, curcumin nanoparticles, *Pseudomonas aeruginosa*, infected wounds, wound healing.

Introduction

The skin, which accounts for 15-20% of an adult's total body weight (1) and performs numerous essential bodily tasks including homeostasis and protection, serves as the body's first line of defense against external, bodily, chemical, and physical aggressors. It is made up of the epidermis, dermis, and subcutaneous tissue in three layers (2, 3).

A wound is a separation and discontinuity in the layers of the skin that

Al-Qadisiyah Journal of Veterinary Medicine Sciences
(P-ISSN 1818-5746/ E-ISSN 2313-4429)
www.qu.edu.iq/journalvm

makes it more susceptible to contamination and infection. The bacteria already present on the skin, such as coagulase-negative species (*Staphylococci*, *Streptococci*, *Bacillus*), and *Corynebacterium* species, can quickly contaminate and infect open wounds. *Pseudomonas aeruginosa* (PA) could be observed to persist in 50% of chronic incurable wounds. The key factors contributing to the difficulties in treating PA in wound infections were the emergence of bacterial biofilms and drug-resistant strains. New therapeutic strategies are accordingly needed to locally eliminate PA and remove its biofilms (4, 5).

Antibiotics are the most dominant treatment for infected wounds. Antibiotics are becoming less effective for bacterial wound infections due to widespread antibiotic misuse and a growing number of multi-resistant bacterial species such as *Pseudomonas aeruginosa* and methicillin-resistant *S. aureus* (6). The therapeutic efficacy of antibiotics is threatened by antimicrobial resistance, posing a concern on a worldwide scale and leading to rising morbidity and mortality (7). The rising and disseminated resistance to antibiotics made mandatory the search for new drugs and/or alternative therapies that are able to eliminate resistant microorganisms and impair the development of new forms of resistance (8).

Turmeric (Curcuma longa) with curcumin as an active ingredient, possesses healing, antibacterial, and natural photosensitizer properties (9,10,11,12,and 13). It has been shown a variety effects on wound healing. It has potent tissue healing modulating properties achieves by working on the inflammatory, proliferative, and remodeling phases of the wound healing process, thereby shortening the time required for wound healing (14,15). Also they display suppressed the growth of methicillin-resistant *Staphylococcus aureus* (MRSA) and *Pseudomonas aeruginosa* in vitro in a dose-dependent manner, as well as MRSA in vivo (16). Unfortunately, curcumin's bioavailability, rapid metabolism, weak solubility, and light sensitivity restrict its potential. Novel formulations, such as nanoparticles, should be investigated in order to reduce these effects and maximize the effectiveness of curcumin (5,17). Fortunately the chemical structure of nanocurcumin was the same as that of curcumin, and no changes were made during nanoparticle production (18). Nanocurcumin was far more efficient than curcumin against *Staphylococcus aureus*, *Bacillus subtilis*, *Escherichia coli*, *Pseudomonas aeruginosa*, *Penicillium notatum*, and *Aspergillus niger* (19, 20, and 21). The study aimed to evaluate the topical application of turmeric extract nanoparticles ointment for treatment of induced *Pseudomonas aeruginosa* infected open wounds in mice.

Materials and Methods

Ethical approval

The current study protocol was approved by the College of Veterinary Medicine, University of Al-Qadisiyah, Al-Diwaniyah, Iraq

Indian dry turmeric rhizomes (C. longa) were purchased from Diwaniyah market. Rhizomes were cleaned, ground into tiny particles in a dry grinder for 20 minutes. The powder was sieving with a mesh size of 212 microns. A 50 gram of turmeric powder placed in the extraction thimble for ethanolic turmeric extraction by Soxhlet apparatus at 60°C for 8 hours. The ethanolic extract placed in Petri dishes until the alcohol evaporates at 50°C, then scraped and processed to create the turmeric powdered extract (22, 23).

Al-Qadisiyah Journal of Veterinary Medicine Sciences
(P-ISSN 1818-5746/ E-ISSN 2313-4429)
www.qu.edu.iq/journalvm

The turmeric extract powder convert to nanoparticles by ultrasonic method (24), A 10 grams of turmeric extract powder was dissolved in 100 ml of ethanol, the solution was filtered three times; two times with a filter paper and the third time was filtered by syringe filters (0.22 nm). The filtered solution was sonicated with Ultrasonic Cell Disruptor device (Ultrasonic Cell Disruptor: UCD-150; Ultrasonic Power 150 W, Probe 6mm) (Faithful Intelligent Ultrasonic Processor), using wave energy 50 watts for 30 minutes, where the turmeric particles in the solution reached 62 nm in size (25, 26). The turmeric extract nanoparticles solution was dried in oven (50℃). The dried extract was collected and grinded to become dry extract nanoparticles powder.

X-Ray Diffraction (XRD), UV Visible Absorption Spectroscopy, Scanning Electron Microscopy (SEM), and Fourier Transform Infrared (FTIR) spectroscopy, were used to evaluate the structural analysis of the turmeric extract nanoparticles (The morphology, shape, size, and surface area).

Turmeric extracts nanoparticles ointment preparation

To get fine, homogenized extract powder particles, the dry turmeric extract nanoparticles were ground into a powder and sieved through a 212 micron mesh size sieve. In order to create the ointment, the base (Vaseline) was triturated with a mortar and pestle, combining the extract powder or extract nanoparticles powder as the active ingredient (27, 28). In a glass mortar, 97 grams of Vaseline and three (3) grams of turmeric extract nanoparticles powder were combined to create a 3% w/w turmeric extract nanoparticles ointment. Tiny amount of pure liquid glycerin was put in the mortar, then the powder was added and well crushed with a pestle to dissolve the contents. A small amount of Vaseline was added, and the mixture was triturated with a pestle. Subsequently, gradually adding more base (Vaseline), and the mixture was again triturated till all the 97 gm. of Vaseline was over and the mixture becomes uniform. To increase the homogeneity of the combination, the mixture was transferred to a container and thoroughly stirred by repeatedly inverting it using a vortex mixer for 10 minutes. The prepared ointment was then placed in a dark container and stored in a room temperature till use (27, 29, and 30).

Experimental design

Thirty adult male mice were utilized. Two open full-thickness (0.5cm in diameter) skin incision on the back of the animal were made. Infection was creating in the right incisions after 24 hrs. from wounding by inoculating of 0.2 mL *Pseudomonas aeruginosa* bacterial suspension containing $2x10^8$ CFU/mL of bacteria. The left incisions not inoculated, and left without treatment as control in the same animal. Animals were randomly divided into two groups (n 15). G1 (Control group) inoculated with bacteria and not treated. The infected wounds of G2 treated with a topical application of 3% turmeric extract nanoparticle ointment in a dose of $30mg/cm^2$ once a day, for 7 successive days.

Morphometric examination (wound area (size of wound), and wound contraction) of wound healing organized by direct measuring of wound dimensions on the 7^{th} and 14^{th} days post infection (PI). When the wound is circular; Circular surface area = $(\text{half diameter})^2 \times 3.14$. When the shape of wound changed; the surface area = Length x Width. The wound contraction was calculated by the following formula: Percentage of wound contraction = (wound area on day 0 - wound area on day n /wound area on day 0 x 100) (31, 32).

Al-Qadisiyah Journal of Veterinary Medicine Sciences
(P-ISSN 1818-5746/ E-ISSN 2313-4429)
www.qu.edu.iq/journalvm

Specimens of healed skin (1 cm^3) were collected after 7 and 14 days PI for histopathological evaluation of the healing process.

For wound bacterial count; the inoculated wounds were swabbed with sterile cotton swabs on the 3rd day after inoculation (1st day of infection) just before application of topical treatment, as well as, swabs were taken at 7th day (PI). Swabs were placed in 1 mL of diluents containing a 0.1% peptone in 0.85% normal saline ratio of 1:99. The initial nutrient broth suspensions and their tenfold serial dilutions (0.1 mL each) were cultured on nutrient agar (according to the pour plate method for bacterial count). Colonies were counted after a 24-hour incubation period at 37 C°. by using Quebec colony counter. The number of bacterial colonies forming units (CFU) per mL of sample was calculated by dividing the number of colonies by the dilution factor and multiplying the result by the volume of a specimen placed on liquefied agar (33).

Results

X-Ray Diffraction (XRD)

The X- Ray diffractogram of turmeric extract nanoparticles displayed a decrease in the number of peaks relative to turmeric extract, indicating a non-crystallized atomic arrangement and shifting into the amorphous phase or lower crystallinity turmeric extract nanoparticles (Fig. 1).

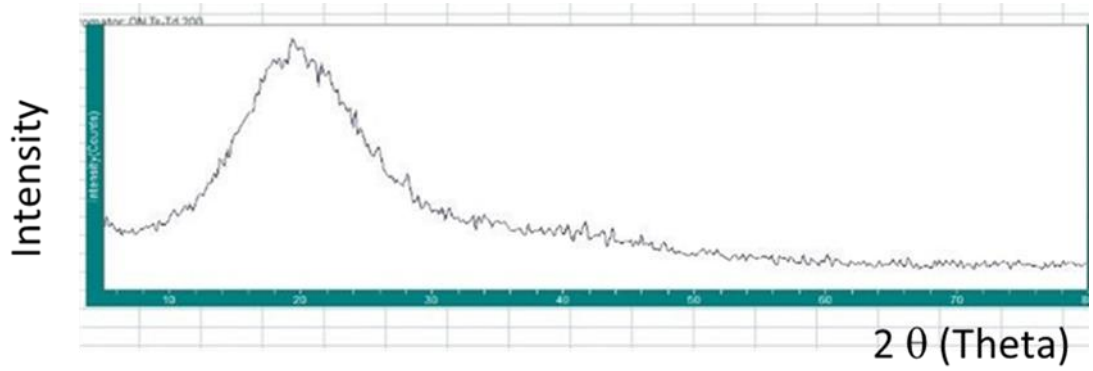

Fig. (1) X- Ray diffractogram of turmeric extract nanoparticles.

UV-Visible Absorption Spectroscopy

The maximum absorption spectra of the turmeric extract nanoparticles were seen shifted from 423 nm to 422 nm wavelength. This result primarily confirmed that turmeric extract nanoparticles were successfully fabricated (Fig. 2).

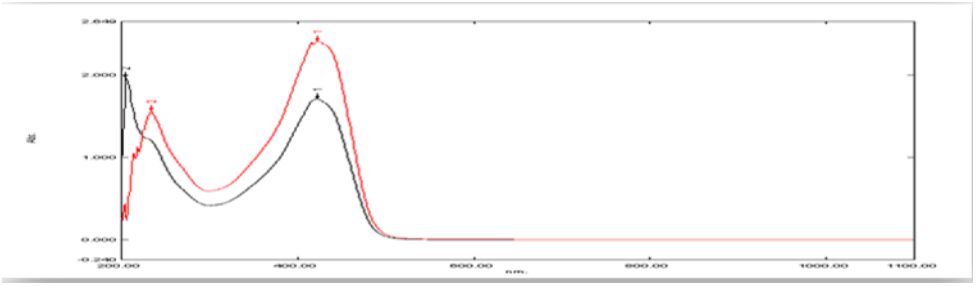

Fig. (2). UV-Visible results show the peaks of absorption at variable wavelengths. Red curve; turmeric extract 423 nm. Black curve; turmeric extracts nanoparticles 422 nm.

Al-Qadisiyah Journal of Veterinary Medicine Sciences
(P-ISSN 1818-5746/ E-ISSN 2313-4429)
www.qu.edu.iq/journalvm

Scanning Electron Microscopy (SEM)

The scanning electron microscopic images of the turmeric extract nanoparticles prepared by ultrasonic technique were found to be smooth amorphous spherical particles in shape ranging from 52 to 91 nm in size (Fig. 3).

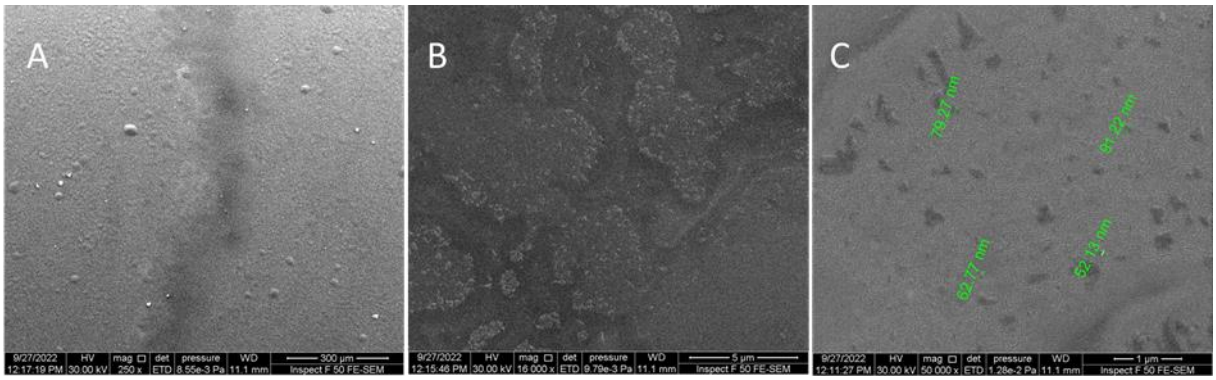

Fig. (3). SEM images of spherical turmeric extract nanoparticles. A. 250X magnification. B. 16000X magnification. C. 50000X magnification.

Fourier Transform Infrared (FTIR) Spectroscopy

The turmeric extract nanoparticles were analyzed using Fourier Transform Infrared Spectroscopy (FTIR) at the mid-infrared region (4000-400 cm^{-1}). The broad, intense band at wavenumber 3384 cm^{-1} corresponds to the stretching vibration of hydrogen-bonded O−H present in turmeric extract nanoparticles. Asymmetric stretching vibrations of Csp2−H and Csp3−H are shown at 2925 and 2853 cm^{-1}, respectively. C−H frequency of the aromatic overtone is obtained at 3009 cm^{-1}. Bands at 1449 and 1377 cm^{-1} correspond to the aromatic stretching vibrations of the benzene ring. The intense characteristic band centered at 1721 cm^{-1} corresponds to the stretching vibration of the conjugated carbonyl (C = O). Stretching vibrations of double-bonded carbon, Csp2−O, and Csp3−O bonds are shown at 1624, 1588, and 1165 cm^{-1}, respectively (Fig. 4).

Al-Qadisiyah Journal of Veterinary Medicine Sciences
(P-ISSN 1818-5746/ E-ISSN 2313-4429)
www.qu.edu.iq/journalvm

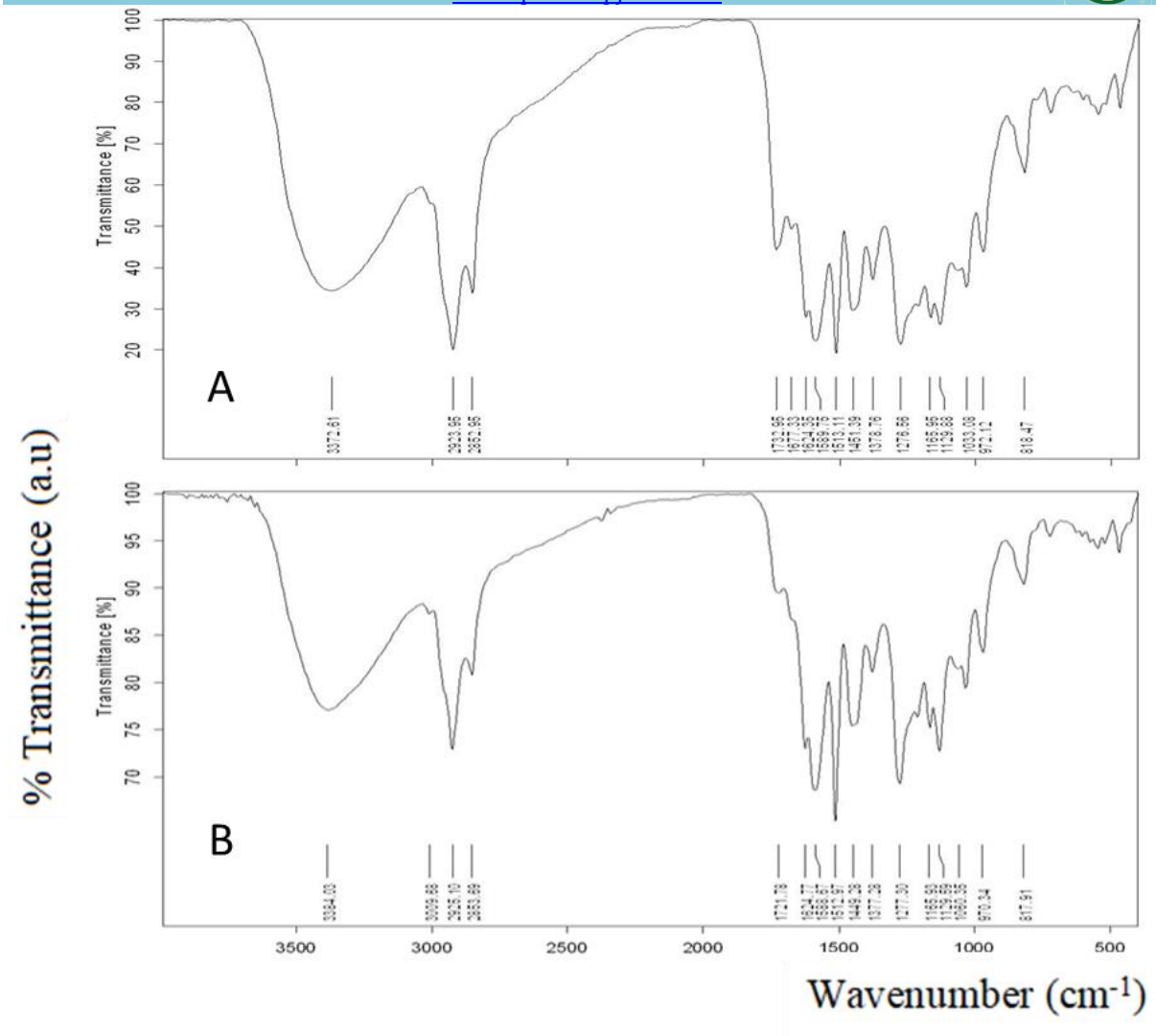

Figure (4). A- FTIR of turmeric extract at (4000−400 cm^{-1}), reveal characteristic peaks at 3372.61 cm^{-1}, 1732.95 cm^{-1}, 1677.33 cm^{-1}, 1280. 65 cm^{-1}, 1029.92 cm^{-1}, 960.48 cm^{-1}, 811.98 cm^{-1} and 717.47 cm^{-1}.;
B- FTIR of turmeric extract nanoparticles (4000-400 cm^{-1}) the peaks at 3384.03 cm^{-1}, 1721.78 cm^{-1}, 1624.77 cm^{-1}, 1588.67 cm^{-1}, 1277.30 cm^{-1}.

Evaluation of antibacterial activity (Wound bacterial count)

Application of turmeric extract nanoparticles against infected wounds at the 1st day PI (3rd post wounding (PW)) show there was a vast bacterial colonies number (uncountable) on both groups, and the bacterial colonies number become countable on the third dilution only. At the 7th day PI (10th day PW) the bacterial colonies number become countable in G2 from the first dilution in compare with G1 (Fig. 5).

Al-Qadisiyah Journal of Veterinary Medicine Sciences
(P-ISSN 1818-5746/ E-ISSN 2313-4429)
www.qu.edu.iq/journalvm

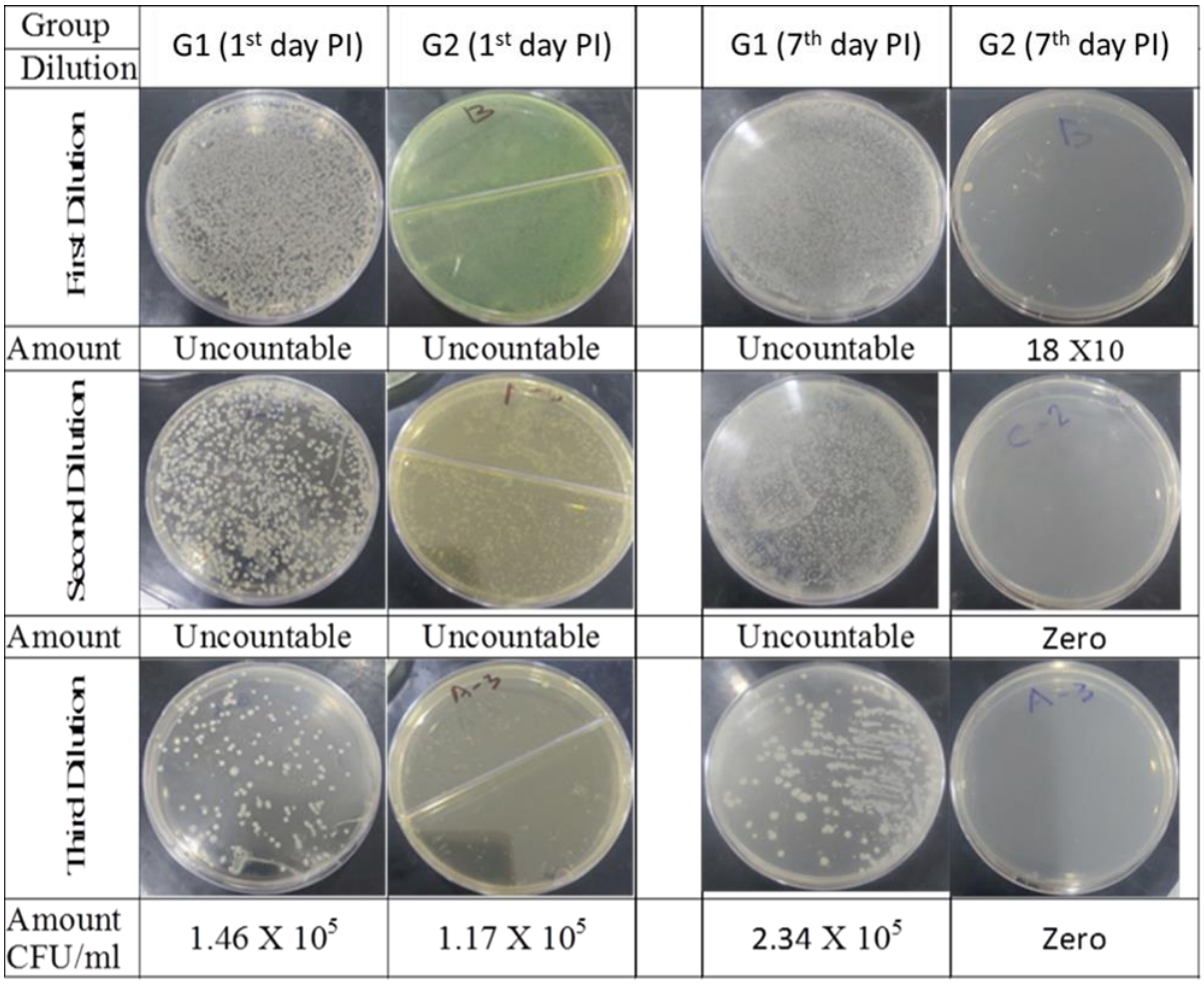

Fig. (5) Antibacterial activity (CFU/mL) of topical application of turmeric extract nanoparticles against infected wounds via *Pseudomonas aeruginosa* in mice, at first and seventh days PI (G1=Control), (G2= Turmeric extracts nanoparticles group).

Morphometric assessment of the wound healing:

Surface area (size of wound)

The initial size of wound (mm^2) on day zero in treated and control wounds was (19.62) mm^2. The size of inoculated (infected non-treated) wounds in G1 (129.35%) were become significantly $P < 0.05$ larger than the original size, while the size of treated wounds were significantly $P < 0.05$ reduced more than 45.25% in G2 at 7 days PI in compare with initial size of wound. At 14 days PI the size of infected non-treated wounds in G1(174.66%) significantly $P < 0.05$ larger than the original size, and the healing did not occur, while in G2 (32.36%) significantly reduction in size was occur (table 1) (fig. 6, 7).

The percentage of wound contraction was significantly increased ($P < 0.05$) in treated wounds at 7^{th} and 14^{th} days as compared with no wound contraction (0%) in G1.

Al-Qadisiyah Journal of Veterinary Medicine Sciences
(P-ISSN 1818-5746/ E-ISSN 2313-4429)
www.qu.edu.iq/journalvm

Table (1); Surface area and wound contraction. (G1=Control), (G2= Turmeric extract nanoparticles group).

Periods	Groups	Surface area (mm^2)		Wound contraction %	
		Treated	Control	Treated	Control
0 day	G1,G2	19.62^{Aa}	19.62^{Aa}	0^{Aa}	0^{Aa}
7 days	G1	25.38^{Ba}	10.2^{Bb}	0^{Aa}	48.01^{Bb}
	G2	8.44^{CDa}	9.53^{Ba}	56.98^{Da}	51.42^{Eb}
14 days	G1	34.27^{Ea}	8.12^{Cb}	0^{Aa}	58.61^{Cb}
	G2	6.53^{Fa}	8^{Cb}	66.71^{Ga}	59.22^{Cb}
LSD(P<0.05)		1.342		3.018	

- Capital letters refers to the vertical statistical comparison, whereas small letters refer to the horizontal statistical comparison.
- Different letters denote to the significant difference at P<0.05, whereas similar letters refer to the no significant difference.

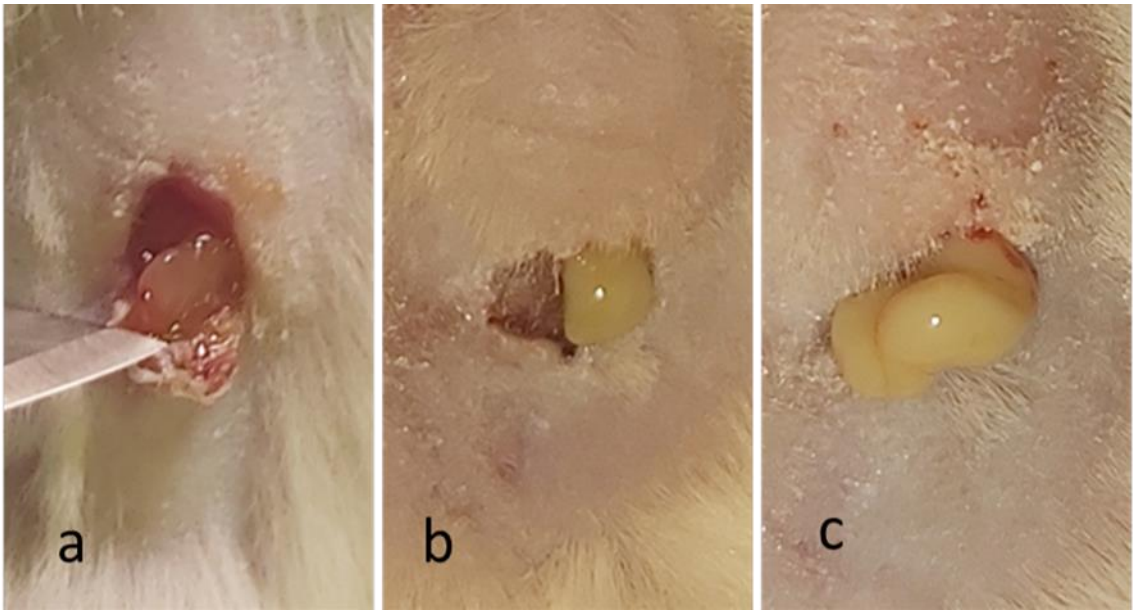

Fig. (6): Macro Photographs of control group (G1); (a)Time zero, (three days after inoculation of *Pseudomonas aeruginosa* in excional wounds), see the early signs of infection, the wound become larger, presence of pus flashing bneath the scab. (b) 7 days PI, see more quantity of pus during reflecting of the scab, the scab became more dry and dark in color. (c) 14 days PI, see a huge quantity of pus creaming out of the wound.

Al-Qadisiyah Journal of Veterinary Medicine Sciences
(P-ISSN 1818-5746/ E-ISSN 2313-4429)
www.qu.edu.iq/journalvm

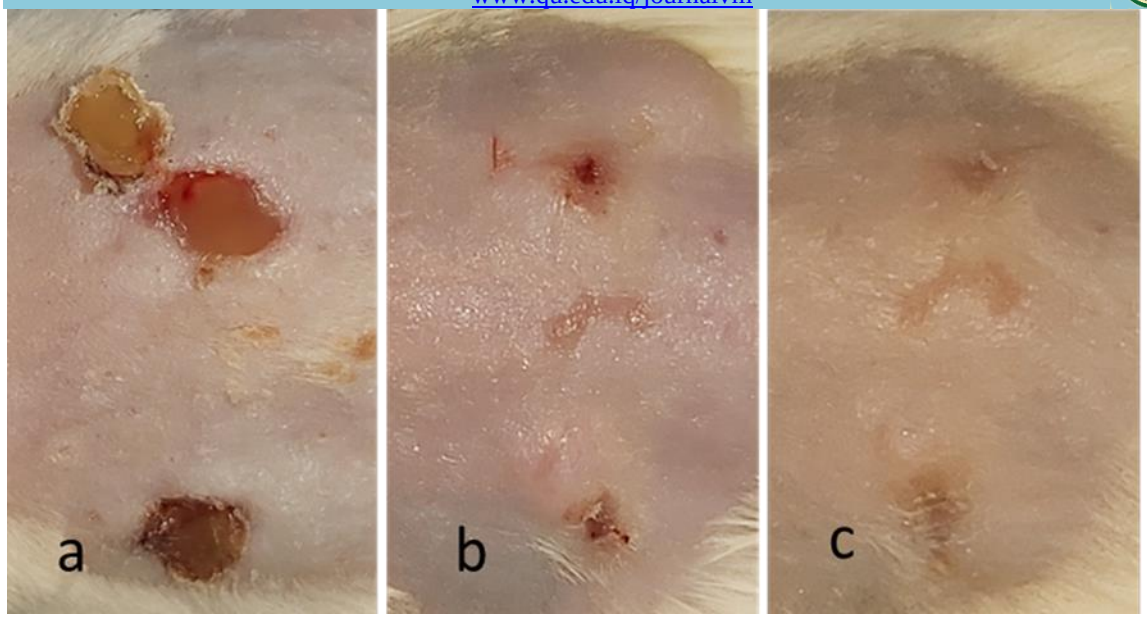

Fig. (7): Macro Photographs of nano-turmeric extract group (G2); (a)Time zero, (three days after inoculation of *Pseudomonas aeruginosa* in cranial wounds (upper)), see the wound become larger, and pus was found below the scab. No signs of infection in the caudal wound (lower) (control wound). (b) 7 days PI and 7 successive days of treatment of the cranial wound (upper) with nano-turmeric extract ointment topically, get complete eradication of infection, good epithelialization, and the wound become small in size than before 7 days.The caudal wound have same size of the cranial, with a thin scab. (c) 14 days PI, see more improvement in epithelilization of treated (cranial) wound, and the wound become more small in size.

Histopathological assessment of the wound healing

Non-infected wounds in G1

The histopathological findings of non-infected (control) skin wounds of G1 at the 7th day PI (7th day PI identical the 10th days post wounding PW) show complete reepithelization (presence of all layers of epidermis), thickening of the epithelial layer at the periphery of the wound, and no scab was found upon the wound. There were dense immature collagen fibers and fibroblasts in the dermis and no inflammatory cells (Fig. 8). While in (14th day PI) shows complete re-epithelization of the epidermis, mature collagen fibers arranged parallel to the epithelium, and myofibroblasts in the dermis, also presence of discrete epithelial cells in the regenerated dermis layer. The panniculus carnosus (PC) muscle was found (Fig. 9).

Infected non-treated wounds in G1

The histopathological outcomes show; absence of epithelial layers, presence of suppurative exudate, dead liquefied tissue, plenty of dead and live polymorphonuclear cells (neutrophils) in the center of wound, and collagen fibers at the periphery of the wound near the intact tissue (Fig. 10). While in 14 days (PI) show no epithelial layers, no signs of the wound healing. The dermis had homogenized field containing massive access of dead and live neutrophils (PMNC) and debris tissue. The periphery of the wound adjacent the healthy tissue had a collagen fibers arranged in an uneven manner, and newly formed blood vessels (Fig. 11).

Infected and treated wounds in G2

The histopathological findings of the infected wound 7th day PI show, no infection, complete epithelialization of epidermis.

Al-Qadisiyah Journal of Veterinary Medicine Sciences
(P-ISSN 1818-5746/ E-ISSN 2313-4429)
www.qu.edu.iq/journalvm

Although absence of infection there was moderate attendance of inflammatory cells, immature granulation tissue, and panniculus carnosus are seen (Fig. 12) while in 14th day PI show, no signs of infection, well regenerated epidemis, the dermis compose dense mature collagen fibers with myofibroblast, and scarce inflammatory cells, sebaceous glands also seen. Superficail and deep dermis (Fig. 13)

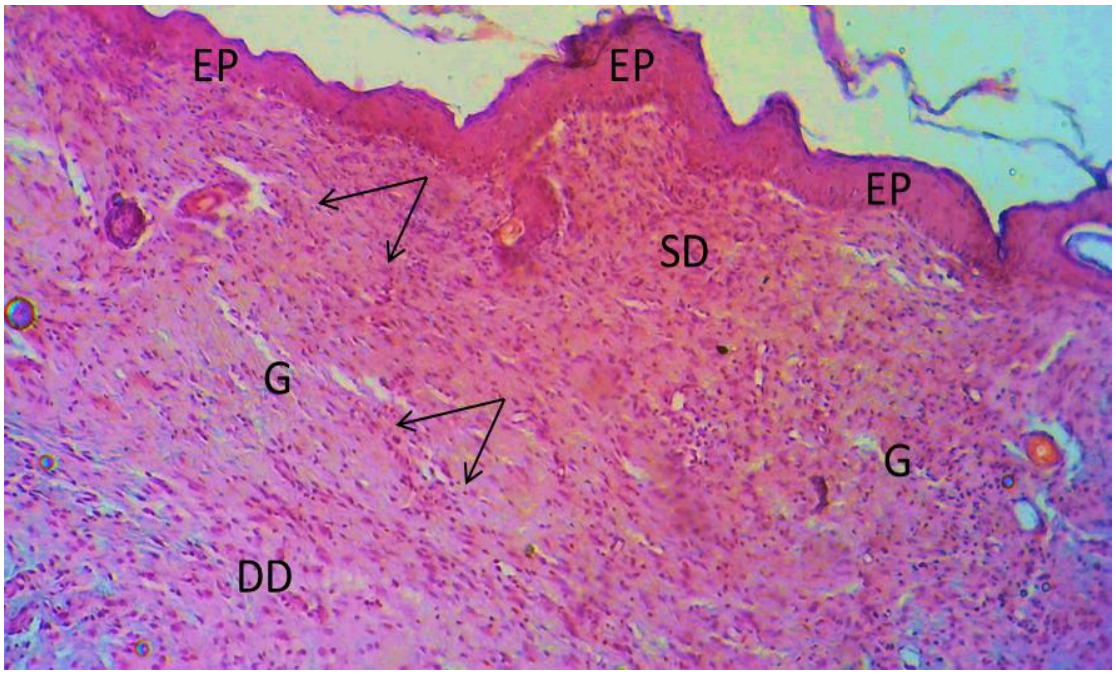

Fig. (8); G1; non-infected wound 10 days PW (7th day PI), shows complete re-epithelization of the epidermis (EP), thickening of the epithelium at the periphery of the wound and presence of immature dense collagen fibers (G) and fibroblasts (black arrows) in the dermis, H&E, 10X

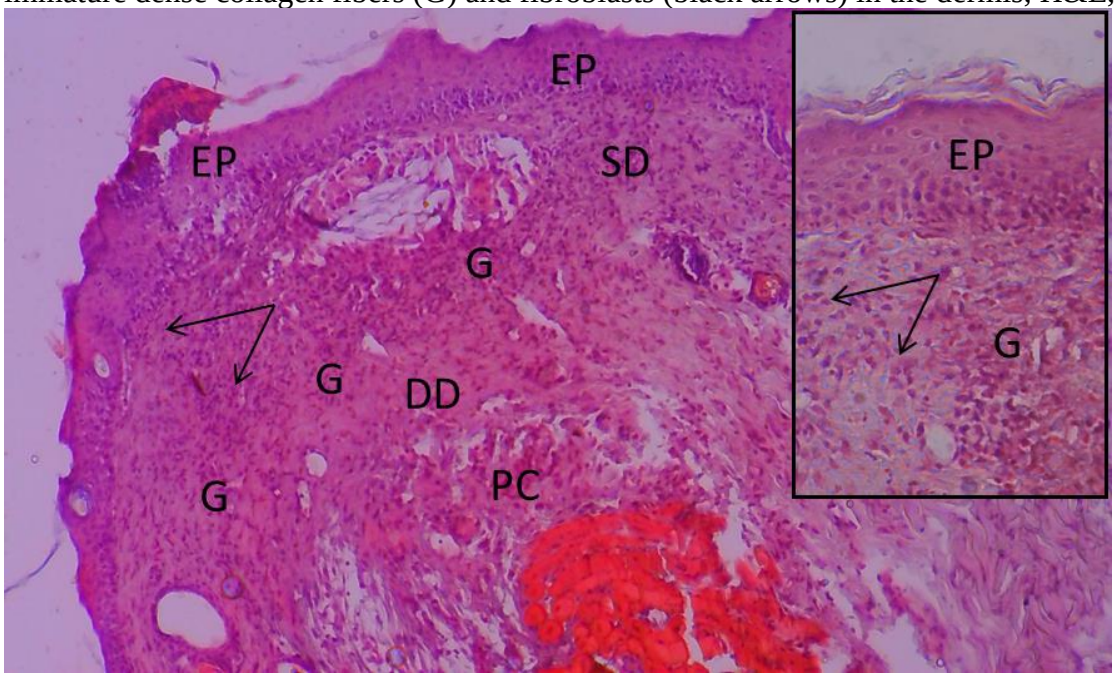

Al-Qadisiyah Journal of Veterinary Medicine Sciences
(P-ISSN 1818-5746/ E-ISSN 2313-4429)
www.qu.edu.iq/journalvm

Fig. (9); G1; non-infected wound 17 days PW (14th day PI), shows regenerated thick epidermis (EP), dense mature collagen fibers (G) fibroblasts (black arrows) and myofibroblasts in the dermis, H&E, 10X. black box H&E, 20X.

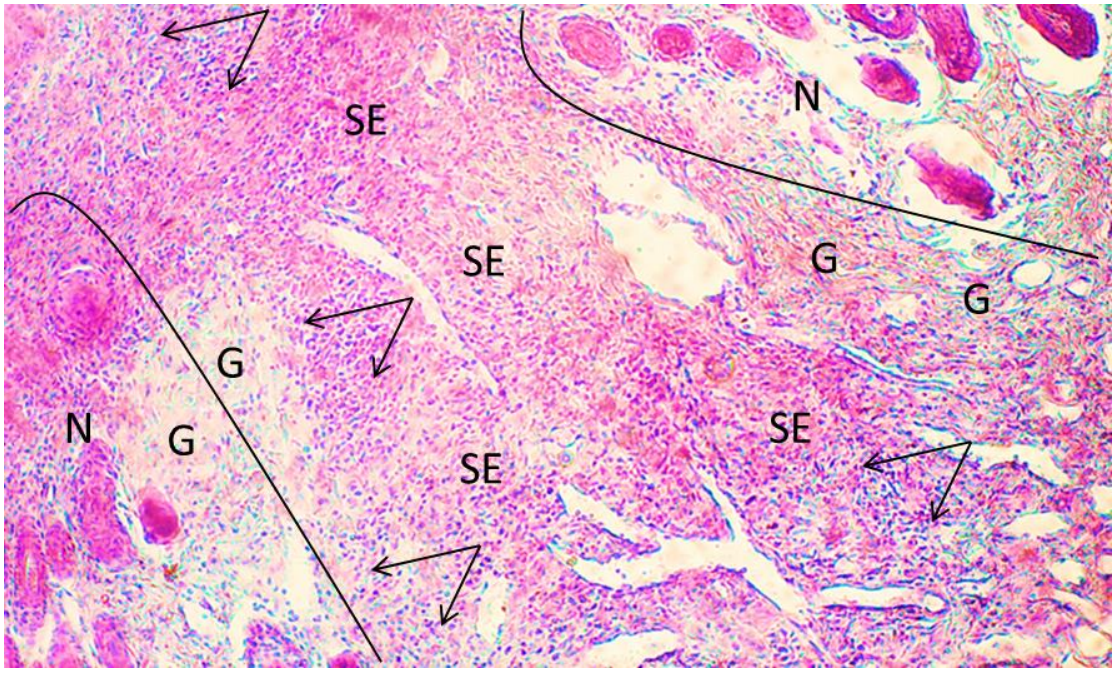

Fig. (10); G1; infected wound 7 days PI, show; absence of epithelial layers, suppurative exudate (SE), dead liquefied tissue, plenty of dead and live neutrophils (black arrow) in the center of wound, and collagen fibers (G) at the periphery of the wound near the entire tissue. H&E, 10X.

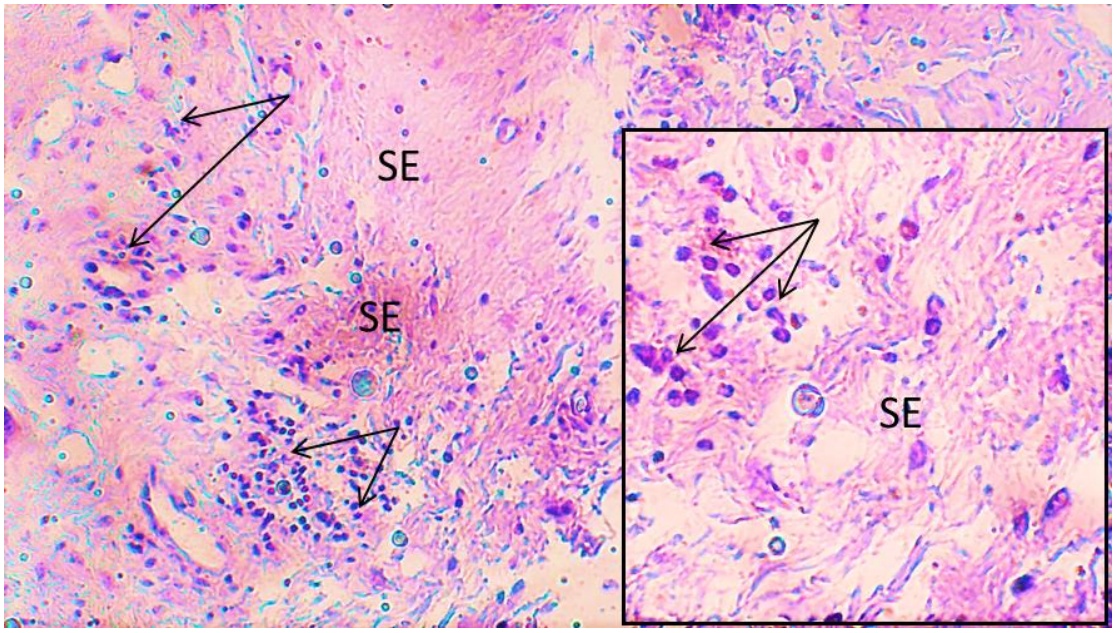

Fig. (11); G1: infected wound 14 days PI, shows massive destruction of the tissue (SE), dead liquefied tissue, plenty of dead, and live neutrophils (black arrows) H&E, 20X. Dead and live neutrophils and debris tissue, H&E, 40X (black box).

Al-Qadisiyah Journal of Veterinary Medicine Sciences
(P-ISSN 1818-5746/ E-ISSN 2313-4429)
www.qu.edu.iq/journalvm

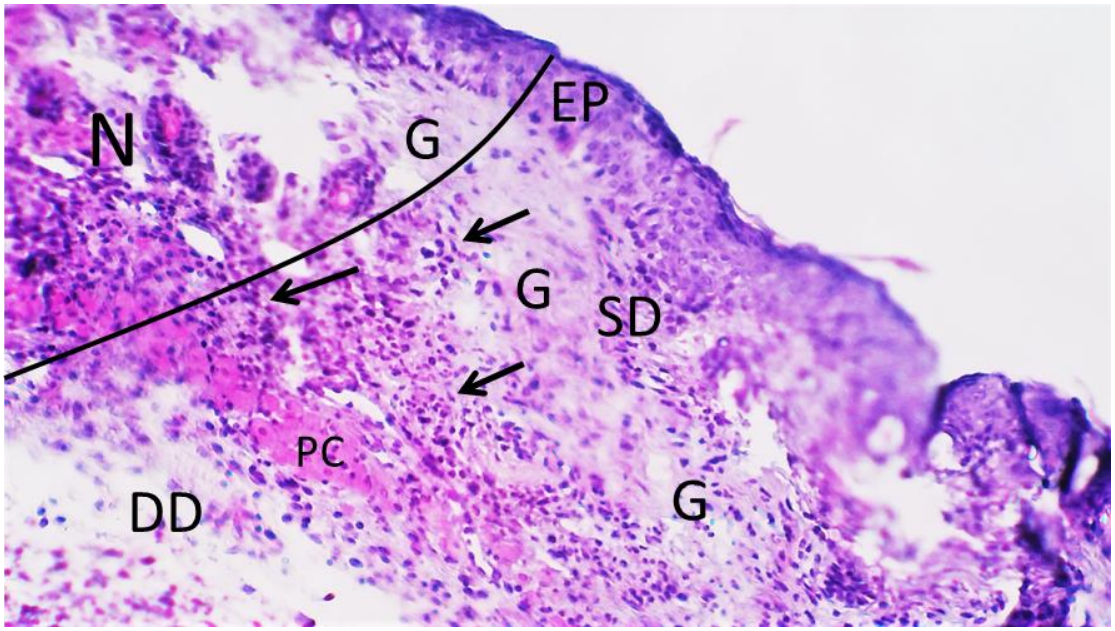

Fig. (12); G2; infected wound 7 days PI show, complete epithelialization of epidermis (EP), moderate attendance of inflammatory cells (black arrows), immature granulation tissue (G), and panniculus carnosus (PC) are seen, H&E, 20X.

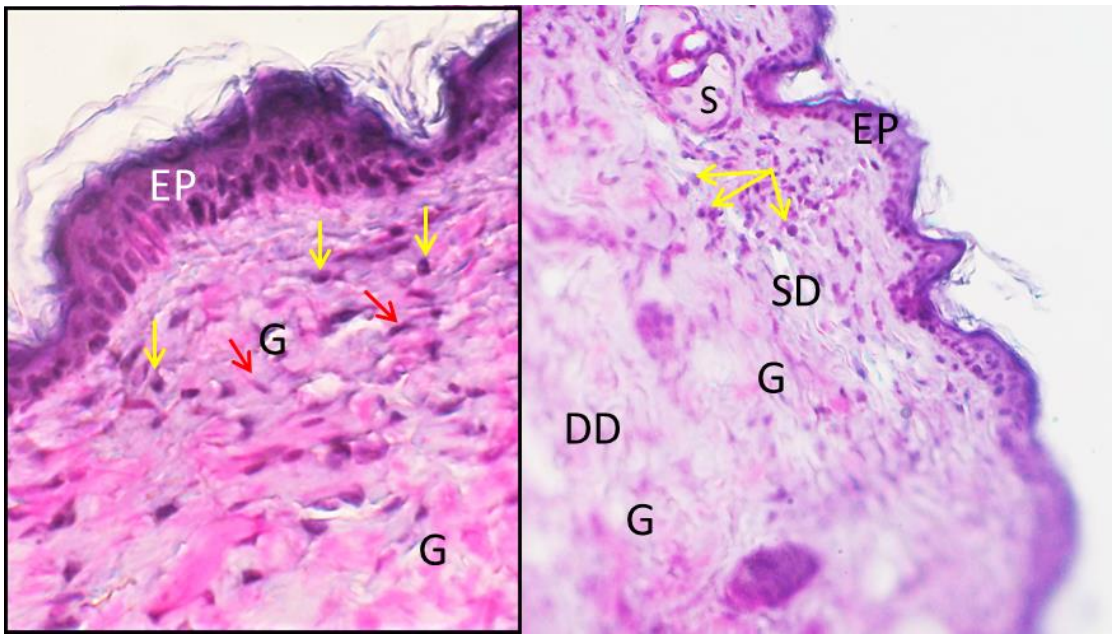

Fig. (13); G2; infected wound 14 days PI show,no signs of infection, well regenerated epidemis (EP), the dermis compose dense mature collagen fibers (G) with myofibroblast (red arrow), and scarce inflammatory cells (yellow arrows), sebaceous glands also seen (S). Superficail dermis (SD), and deep dermis (DD). H&E, 20X. black box 40X.

Al-Qadisiyah Journal of Veterinary Medicine Sciences
(P-ISSN 1818-5746/ E-ISSN 2313-4429)
www.qu.edu.iq/journalvm

Discussion

Turmeric (Curcumin's) limited aqueous solubility and quick degradation profile limit its use; nanoparticle encapsulation overcomes this limitation and allows for longer topical delivery of curcumin (34, 35, and 36). Nanotechnology has proven to be an excellent strategy for accelerating wound healing by inducing proper mobility during various healing phases (15). Many studies indicating that curcumin has remarkable anti-inflammatory, antioxidant, and anti-infective activity, as well as hastening the healing process by acting at various stages of the wound healing process, but its poor biopharmaceutical properties (low aqueous solubility and skin penetrability) limit its therapeutic efficacy for skin applications (18, 37, 38). Therefore, we had to find a way to speed up its work, so it was converted into Nano through the sonicator device, where it was not effect on chemical composition when it was examined with some tests (18).

The amorphous structure of turmeric extract nanoparticles shown by the XRD data indicated a non-crystallized atomic arrangement**,** indicating successful conversion of the extract to nanoparticles which is consistent with earlier researches (39,40). The smooth and spherical surfaces turmeric extract nanoparticles ranged from 52 to 91 nm observed by SEM in this study is in accordance with (39, 41). The UV- Visible results represented the peaks of absorption of the turmeric extract at 423 nm wavelength and the absorption of the Nano turmeric extract at 422 nm wavelength, which indicate the successful fabrication of turmeric extract nanoparticles. This result was in consistent with earlier researches (40, 41). FTIR is a technique it can indicate a specific attribute of the chemical bond and molecular structure of the material. A distinct molecular structures and chemical bonding's imprint can be found in the FTIR peaks and spectrum (42, 43).

Results show uncountable number of bacterial colonies in the first dilution at the 3rd day PI (First day of treatment) in all treated wounds, where it becomes countable only on the third dilution. At day 7 PI, The bacterial numbers become zero in G2 since the second dilution at the 7th day PI. This gain result was almost identical to what was reached by (44) who proved the efficiency of Nano-curcumin in reducing the number of bacteria. The size of treated infected wound in (G2) At 7 days PI was significantly reduced more than 50% than the original size. At 14 days PI, the reduction in size become significantly more where it reach to(32.36)%. While in G1 show No signs of healing was seen in non-treated infected wounds (infected control). The wound size were become significantly $P < 0.05$ larger than the original size at 7 and 14 days PI, with no wound contraction. At the 14 days PI the size of non-treated infected wounds is 174.66% significantly $P < 0.05$ larger than the original size. The inoculated wounds exhibit pus discharging at 7 days PI, and the pus become more worse at 14 days PI. This result is according with (45), they found increase the size of wound, presence of pus and exaggeration of infection. Infections with bacteria are very harmful to wound healing, especially if the wound already has delayed wound healing (46). Bacterial infections slow down the wound healing process by prolonging the inflammatory phase (47).

Results of this study are in line with those of (19), who exposed that Nano curcumin aqueous dispersion was far more effective than curcumin against Staphylococcus aureus, Bacillus subtilis, Escherichia coli, Pseudomonas aeruginosa, and Candida albicans. His findings also show that particle size reduction up to the Nano range significantly improves curcumin's water solubility and antibacterial effectiveness. The activity of Nano curcumin against Gram-positive bacteria was stronger than against Gram-negative bacteria for the selected species. Furthermore, its antibacterial efficacy outperformed its antifungal activity. Transmission electron microscopy (TEM) research was used to explore the mechanism of antibacterial action of curcumin

Al-Qadisiyah Journal of Veterinary Medicine Sciences
(P-ISSN 1818-5746/ E-ISSN 2313-4429)
www.qu.edu.iq/journalvm

nanoparticles, which demonstrated that these particles entered the bacterial cell by fully shattering the cell wall, resulting in cell death.

Conflict of interest

There is no conflict of interest

References

1 .Mescher AL. Junqueira's Basic Histology Text and Atlas. Chapter (18), Skin. 15th ed. New York: McGraw Hill; 2018. p. 371-392.
2 .Garcia JGM. The Role of Photodynamic Therapy in Wound Healing and Scarring in Human Skin. PhD Thesis; The University of Manchester; 2015.
3 .Nafisi S, Maibach HI. Skin penetration of nanoparticles. In: Shegokar R, Souto EB, editors. Emerging Nanotechnologies in Immunology, The Design, Applications and Toxicology of Nanopharmaceuticals and Nanovaccines. Micro and Nano Technologies, 1st ed. Amsterdam: Elsevier; 2018. p. 47-88. https://doi.org/10.1016/B978-0-323-40016-9.00003-8
4 .Lei X, Liu B, Huang Z, Wu J. A clinical study of photodynamic therapy for chronic skin ulcers in lower limbs infected with Pseudomonas aeruginosa. Arch Dermatol Res. 2015;307(1):49-55. https://doi.org/10.1007/s00403-014-1520-4
5 .Mirzahosseinipour M, Khorsandi K, Hosseinzadeh R, Ghazaeian M, Shahidi FK. Antimicrobial photodynamic and wound healing activity of curcumin encapsulated in silica nanoparticles. Photodiagnosis Photodyn Ther. 2020;29:101639. https://doi.org/10.1016/j.pdpdt.2019.101639
6 .Kant V, Gopal A, Kumar D, Pathak NN, Ram M, Jangir BL, et al. Curcumin-induced angiogenesis hastens wound healing in diabetic rats. J Surg Res. 2015;193(2):978-988. https://doi.org/10.1016/j.jss.2014.10.019
7 .Akasov R, Khaydukov EV, Yamada M, Zvyagin AV, Leelahavanichkul A, Leanse LG, et al. Nanoparticle enhanced blue light therapy. Adv Drug Deliv Rev. 2022;184:114198. https://doi.org/10.1016/j.addr.2022.114198
8 .de Freitas LF, Hamblin MR. Proposed mechanisms of photobiomodulation or low-level light therapy. IEEE J Sel Top Quantum Electron. 2016;22(3):348-364. https://doi.org/10.1109/JSTQE.2016.2561201
9 .Kulac M, Aktas C, Tulubas F, et al. The effects of topical treatment with curcumin on burn wound healing in rats. J Mol Histol. 2013;44(1):83-90. https://doi.org/10.1007/s10735-012-9452-9
10 .Akbik D, Ghadiri M, Chrzanowski W, Rohanizadeh R. Curcumin as a wound healing agent. Life Sci. 2014;116(1):1-7. https://doi.org/10.1016/j.lfs.2014.08.016
11 .Gunes H, Gulen D, Mutlu R, Gumus A, Tas T, Topkaya AE. Antibacterial effects of curcumin: an in vitro minimum inhibitory concentration study. Toxicol Ind Health. 2013;32(2):246-250. https://doi.org/10.1177/0748233713498458
12 .Ghorbani J, Rahban D, Aghamiri S, Teymouri A, Bahador A. Photosensitizers in antibacterial photodynamic therapy: An overview. Laser Ther. 2018;27(4):293-302. https://doi.org/10.5978/islsm.27_18-RA-01
13 .Trigo-Gutierrez JK, Vega-Chacón Y, Soares AB, Mima EGDO. Antimicrobial activity of curcumin in nanoformulations: a comprehensive review. Int J Mol Sci. 2021;22(13):7130. https://doi.org/10.3390/ijms22137130
14 .Mohanty C, Sahoo SK. Curcumin and its topical formulations for wound healing applications. Drug Discov Today. 2017;22(10):1582-1592. https://doi.org/10.1016/j.drudis.2017.07.001
15 .Kumari A, Raina N, Wahi A, et al. Wound-Healing Effects of Curcumin and Its Nanoformulations: A Comprehensive Review. Pharmaceutics. 2022;14(11):2288. https://doi.org/10.3390/pharmaceutics14112288
16 .Lopes LQS, De Souza ME, Vaucher RDA, Santos RCV. Antimicrobial Activity of Nanotechnological Products. In: Drug Delivery Approaches and Nanosystems. Apple Academic Press; 2017. p. 361-381.
17 .Salehi B, Rodrigues CF, Peron G, et al. Curcumin nanoformulations for antimicrobial and wound healing purposes. Phytother Res. 2021;35(5):2487-2499. https://doi.org/10.1002/ptr.6976
18 .Hettiarachchi SS, Dunuweera SP, Dunuweera AN, Rajapakse RG. Synthesis of curcumin nanoparticles from raw turmeric rhizome. ACS Omega. 2021;6(12):8246-8252. https://doi.org/10.1021/acsomega.0c06314
19 .Basniwal RK, Buttar HS, Jain VK, Jain N. Curcumin nanoparticles: preparation, characterization, and antimicrobial study. J Agric Food Chem. 2011;59(5):2056-2061. https://doi.org/10.1021/jf104402t
20 .Lu Y, Ding N, Yang C, Huang L, Liu J, Xiang G. Preparation and in vitro evaluation of a folate-linked liposomal curcumin formulation. J Liposome Res. 2012;22(2):110-119. https://doi.org/10.3109/08982104.2011.627514
21 .Pandit RS, Gaikwad SC, Agarkar GA, Gade AK, Rai M. Curcumin nanoparticles: physico-chemical fabrication and its in vitro efficacy against human pathogens. 3 Biotech. 2015;5:991-997. https://doi.org/10.1007/s13205-015-0302-9
22 .Patil SS, Bhasarkar S, Rathod VK. Extraction of curcuminoids from Curcuma longa: comparative study between batch extraction and novel three phase partitioning. Prep Biochem Biotechnol. 2019;49(4):407-418. https://doi.org/10.1080/10826068.2019.1575859

Al-Qadisiyah Journal of Veterinary Medicine Sciences
(P-ISSN 1818-5746/ E-ISSN 2313-4429)
www.qu.edu.iq/journalvm

23 .Jiang T, Ghosh R, Charcosset C. Extraction, purification and applications of curcumin from plant materials: A comprehensive review. Trends Food Sci Technol. 2021;112:419-430. https://doi.org/10.1016/j.tifs.2021.04.015

24 .Dhivya S, Rajalakshmi AN. A Review on the preparation methods of Curcumin Nanoparticles. PharmaTutor. 2018;6(9):6-10. https://doi.org/10.29161/PT.v6.i9.2018.6

25 .Rai M, Pandit R, Gaikwad S, Yadav A, Gade A. Potential applications of curcumin and curcumin nanoparticles: From traditional therapeutics to modern nanomedicine. Nanotechnol Rev. 2015;4(2):161-172. https://doi.org/10.1515/ntrev-2015-0001

26 .Aldulemy QLM, Abdul-Razak MMA. Effect of Nano Seaweed Extract on Tillaring Pattern, growth and yield of Barley Varieties. Int J Aquat Sci. 2021;12(2):5385-5400.

27 .Chhetri HP, Yogol NS, Sherchan J, et al. Formulation and evaluation of antimicrobial herbal ointment. Kathmandu Univ J Sci Eng Technol. 2010;6(1):102-107. https://doi.org/10.3126/kuset.v6i1.3317

28 .Sharma S, Singh SP. Dermatological preparations, formulation and evaluation of various semi-solid dosage form. Asian J Pharm Res Dev. 2014;2:10-25.

29 .Marriott JF, Wilson KA, Langley CA, Belcher D. Pharmaceutical Compounding and Dispensing. 2nd ed. London: Pharmaceutical Press; 2010. p. 163.

30 .Lane ME. Ointments, pastes, gels, cutaneous patches and topical sprays. In: Taylor KM, Aulton ME, editors. Aulton's Pharmaceutics: The Design and Manufacture of Medicines. 6th ed. London: Elsevier Health Sciences; 2022. p. 453-462.

31 .Sardari K, Dehgan MM Mohri M, et al. Macroscopic aspects of wound healing (contraction and epithelialization) after topical administration of allicin in dogs. Comp Clin Pathol. 2006;15(4):231-235. https://doi.org/10.1007/s00580-006-0634-2

32 .Patil MVK, Kandhare AD, Bhise SD. Pharmacological evaluation of ethanolic extract of Daucus carota Linn root formulated cream on wound healing using excision and incision wound model. Asian Pac J Trop Biomed. 2012;2(2):S646-S655. https://doi.org/10.1016/S2221-1691(12)60290-1

33 .Cappuccino JG, Welsh C. Microbiology A Laboratory Manual. 11th ed. England: Pearson Education Limited; 2018. p. 147-155.

34 .Ghalandarlaki N, Alizadeh AM, Ashkani-Esfahani S. Nanotechnology-applied curcumin for different diseases therapy. Biomed Res Int. 2014;2014:394264. https://doi.org/10.1155/2014/394264

35 .Abirami M, Raja J, Mekala P, Visha P. Preparation and characterisation of nanocurcumin suspension. Int J Sci Environ Technol. 2018;7(1):100-103.

36 .Duong BH, Truong HN, Phan Nguyen QA, et al. Preparation of curcumin nanosuspension with gum arabic as a natural stabilizer: Process optimization and product characterization. Processes. 2020;8(8):970. https://doi.org/10.3390/pr8080970

37 .Wang S, Tan M, Zhong Z, et al. Nanotechnologies for curcumin: an ancient puzzler meets modern solutions. J Nanomater. 2011;2011:631357. https://doi.org/10.1155/2011/723178

38 .Algahtani MS, Ahmad MZ, Nourein IH, et al. Preparation and characterization of curcumin nanoemulgel utilizing ultrasonication technique for wound healing: In vitro, ex vivo, and in vivo evaluation. Gels. 2021;7(4):213. https://doi.org/10.3390/gels7040213

39 .Rachmawati H, Yanda YL, Rahma A, Mase N. Curcumin-loaded PLA nanoparticles: formulation and physical evaluation. Scientia Pharmaceutica. 2016;84(1):191-202. https://doi.org/10.3797/scipharm.ISP.2015.10

40 .Wu J, Chen J, Wei Z, et al. Fabrication, Evaluation, and Antioxidant Properties of Carrier-Free Curcumin Nanoparticles. Molecules. 2023;28(3):1298. https://doi.org/10.3390/molecules28031298

41 .Rahman M, Singh JG, Afzal O, et al. Preparation, Characterization, and Evaluation of Curcumin-Graphene Oxide Complex-Loaded Liposomes against Staphylococcus aureus in Topical Disease. ACS Omega. 2022;7(48):43499-43509. https://doi.org/10.1021/acsomega.2c03940

42 .Nandiyanto ABD, Oktiani R, Ragadhita R. How to read and interpret FTIR spectroscope of organic material. Indones J Sci Technol. 2019;4(1):97-118. https://doi.org/10.17509/ijost.v4i1.15806

43 .Nandiyanto ABD, Ragadhita R, Fiandini M. Interpretation of Fourier Transform Infrared Spectra (FTIR): A Practical Approach in the Polymer/Plastic Thermal Decomposition. Indones J Sci Technol. 2023;8(1):113-126. https://doi.org/10.17509/ijost.v8i1.53297

44 .Krausz AE, Adler BL, Cabral V, et al. Curcumin-encapsulated nanoparticles as innovative antimicrobial and wound healing agent. Nanomedicine. 2015;11(1):195-206. https://doi.org/10.1016/j.nano.2014.09.004

45 .Dakhal MA, Abid TA. Use of Povidone Iodine plus Diode Laser for Treatment of Infected Wound in Mice. Al-Qadisiyah J Vet Med Sci. 2022;21.(2)

46 .Gompelman M, van Asten SA, Peters EJ. Update on the role of infection and biofilms in wound healing: pathophysiology and treatment. Plast Reconstr Surg. 2016;138(3S):61S-70S. https://doi.org/10.1097/PRS.0000000000002679

47 .Wolcott RD, Rhoads DD, Dowd SE. Biofilms and chronic wound inflammation. J Wound Care. 2008;17(8):333-341. https://doi.org/10.12968/jowc.2008.17.8.30796